Journal of Colloid and Interface Science 531 (2018) 47–55

Contents lists available at ScienceDirect

Journal of Colloid and Interface Science

journal homepage: www.elsevier.com/locate/jcis

Regular Article

Amorphous carbon layer: An effective assistant for realizing near-infrared-activated photocatalysis

Yuanyuan Zhang [a], Lili Wang [a], Xiumei Ma [c], Manli Yang [a], Haiyan Jiang [a], Lin Li [a], Chuancong Yuan [a], Jinsheng Shi [a,b,*]

[a] Department of Chemistry and Pharmaceutical Science, Qingdao Agricultural University, PR China
[b] Qingdao Bona Biomimetic Composite Research Institute Co. Ltd., PR China
[c] Electron Microscopy Laboratory, School of Physics, Peking University, PR China

GRAPHICAL ABSTRACT

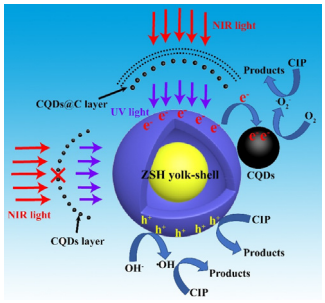

ARTICLE INFO

Article history:
Received 23 May 2018
Revised 11 July 2018
Accepted 11 July 2018

Keywords:
CQDs
Amorphous carbon layer
Up-conversion reason
$ZnSn(OH)_6$
Near-infrared-activated photocatalysis

ABSTRACT

Carbon quantum dots (CQDs) were considered as desirable up-conversion luminescent materials. However, the reason leading to their up-conversion luminescence was not clear. In this paper, CQDs decorated $ZnSn(OH)_6$ was successfully synthesized by facile *in situ* hydrothermal method. Under NIR light irradiation, ciprofloxacin degradation efficiency of sample was 37.4%. Subsequently, reasons for the up-conversion effect of CQDs were investigated to some extent. An amorphous carbon layer around CQDs was observed in composite ($ZnSn(OH)_6$@CQDs@C) by HR-TEM and elemental mapping images. To study the effect of amorphous carbon layer on up-conversion performance, individual CQDs decorated $ZnSn(OH)_6$ ($ZnSn(OH)_6$@CQDs) was also fabricated by compositely coating. $ZnSn(OH)_6$@CQDs had no up-conversion luminescence under 980 nm laser light excitation and its photocatalytic activity was negligible, implying amorphous carbon layer played a crucial role for realizing of up-conversion luminescence. A comparison of the FTIR spectra of two composites, $ZnSn(OH)_6$@CQDs@C sample revealed greatly enhanced surface oxidation degree, polarity and hydrophilicity. Surface state of $ZnSn(OH)_6$@CQDs@C composite was controlled by adjusting hydrothermal time, and the results confirmed that up-conversion performance had a close relationship with surface states of samples. This work could provide a new insight into understanding the up-conversion effect of CQDs.

1. Introduction

With rapid development of social economy, especially acceleration of the process of industrialization, wastewater pollution has become a great threat to aquatic life, human survival and social

* Corresponding author at: Qingdao Agricultural University, Department of Chemistry and Pharmaceutical Science, Chengyang District, Qingdao, PR China.
E-mail address: jsshiqn@aliyun.com (J. Shi).

https://doi.org/10.1016/j.jcis.2018.07.041
0021-9797/

development [1–3]. Millions of serious illness and even death are caused every year by them [4]. Therefore, it is urgently needed to develop rapid and efficient water purification techniques to solve this global challenge [5]. Photocatalysis, as an efficient, low cost and environmentally friendly strategy, has been emerged a preferable candidate in comparison with traditional purification methods [6,7].

In recent years, perovskite materials have attracted widespread interest in organic pollutants photodegradation as well as water splitting for hydrogen production [8,9]. Zinc hydroxystannate ($ZnSn(OH)_6$, ZSH), as one of the perovskite materials, is tended to generate face-centered-cubic crystal structure and filled with hydroxyl groups on surface [10,11]. Much attention has been paid to potential applications of ZSH in photocatalytic process due to its high and stable activity. The efficient photocatalytic performance is assigned to abundant surface OH^- groups, which utilize photoinduced holes to form highly active ·OH radicals. The simple regeneration process of ·OH adducts includes participation of $\cdot O_2^-$ and H_2O [12]. Unfortunately, ZSH could only utilize UV light owing to its wide band gap of 4.0 eV, which only occupies 5% of solar spectrum, whereas residual 45% visible light and 50% NIR light could not be utilized effectively [13]. Among various modified method, morphology control and up-conversion materials decoration could be two effective strategies. On the one hand, based on the reported papers, materials with yolk-shell structures displayed strengthened photocatalytic activity in comparison with hollow and solid counterparts owing to their multi-reflections of light, organic pollutant excellent and light adsorption efficiency [14–16]. On the other hand, carbon is a readily available and low-cost material with nontoxic benefits, which is usually utilized as both supports and metal-free co-catalysts [17,18]. Recently, CQDs, as a newly developed zero-dimensional nanomaterial with sp^2 carbon structure, have been widely applied in photocatalysis [19,20]. Compared to traditional up-conversion (UC) materials doped with rare earth ions, light response of CQDs is not limited to a specific wavelength because of their wide cross-section of UC absorption and a large range of emission spectra that promote energy band-gap matching [21–23]. The unique characters of CQDs such as excellent electrical conductivity, high aqueous solubility, tunable photoluminescence (PL) emissions, environmental friendliness, high chemical stability and earth abundance enable their applications in nanomedicine, bioimaging, biosensing and photocatalysis [24–27]. In particular, CQDs are excellent spectral harvesters and converters due to a wide range of UC absorption and a large cross-section of PL emission spectra, which could convert NIR light to visible and/or UV light through multiple photon absorption [28–30]. In addition, CQDs are also demonstrated to be an excellent electron reservoir to capture photogenerated electrons and inhibit recombination of charge carriers, thereby increasing their lifetimes [24,31].

Herein, $ZnSn(OH)_6$@CQDs and $ZnSn(OH)_6$@CQDs@C microspheres with yolk-shell structure were successfully synthesized by compositely coating and *in situ* hydrothermal method, respectively. PL spectra proved that individual CQDs have no UC character toward 980 nm laser light. Interestingly, self-assembly amorphous carbon could assist CQDs to realize UC luminescence and further driven ZSH-based photocatalytic activity. FTIR and PL spectra suggested that surface states of samples might control the up-conversion luminescence performance This work could provide a new insight into understanding the up-conversion effect of CQDs.

2. Experimental section

2.1. Fabrication of ZSH@CQDs@C composite

ZSH sample with yolk-shell structure was prepared through a facile surfactant-assistant solvothermal method and etching-second growth strategy. The detailed description is presented in Supporting Information. Subsequently, the obtained ZSH as precursor was utilized to fabricate ZSH@CQDs@C composite (Fig. 1a). Typically, 100 mg of ZSH were dispersed into 40 mL deionized water and sonicated for 30 min. After that, 360 mg glucose and 35 mg ascorbic acid were added into the above dispersion with magnetic stir for 30 min. Then the hybrids were transferred to 100-mL Teflon-lined stainless steel autoclaves and heated to 180 °C for 12 h. After cooling to room temperature, precipitate was collected by centrifuge and washed several times with deionized water and ethanol. Final products were dried at 60 °C overnight for further characterization.

Supplementary data associated with this article can be found, in the online version, at https://doi.org/10.1016/j.jcis.2018.07.041.

Pure CQDs (only using 360 mg of glucose and 35 mg of ascorbic acid) was fabricated by the same method. ZSH@CQDs composite was also synthesized by a facile hydrothermal method (Fig. 1b). The detailed description is presented in Supporting Information.

3. Results and discussion

3.1. Morphology and microstructure analysis

Scanning electron microscopy (SEM) and transmission electron microscopy (TEM) are useful technologies to investigate morphology and microstructure of as-prepared samples. As shown in Fig. 2a, ZSH precursor spheres with a smooth surface is uniform and the average size is about 1.3 μm. TEM image in Fig. S1a confirms their solid structure. In the formation of ZSH with yolk-shell structure, ZSH dissolution mainly happen between passivated outer surface of pre-grown seed particles and repeatedly deposited crystal layers, resulting in the generation of yolk-shell structure. As can be seen from Fig. 2b, solid spheres as seed could be preserved well after generation of new shell. In addition, as shown in Fig. S1b, obvious contrast of dark edges and pale center can be clearly seen, suggesting yolk-shell internal structure with a solid yolk. In construction process of CQDs decorated ZSH samples, glucose and ascorbic acid are utilized as a carbon source and acid catalyst for synthesis of CQDs, respectively. Fig. S1c presents the HR-TEM image of CQDs and their average diameters are about 4–5 nm. SEM image in Fig. 2c and TEM images in S1d suggest uniform spherical structure preserved well after modification of CQDs. When ZSH, glucose and ascorbic acid are mixed together, both CQDs and self-assembly amorphous carbon layers are simultaneously formed and surround ZSH microspheres after hydrothermal process. SEM images (Fig. 2d) and TEM images (Fig. 3a) of ZSH@CQDs@C suggest that uniform sphere morphology is perfectly maintained after modification of double carbon layers. Fig. 3b are cross-sectional compositional line profile of ZSH@CQDs@C, which further confirms the yolk-shell structure. Besides, in Fig. 3c, it could be clearly observed that ZSH sample is encapsulated by a self-assembly CQDs layer and intrinsic morphology of CQDs is provided by their HR-TEM images (Fig. 3d). Lattice spacing of CQDs is 0.23 nm and agrees well with (1 0 0) lattice planes of graphite, suggesting CQDs have a crystalline graphitic carbon structure. Furthermore, another amorphous carbon layer arranged over CQDs layer could be clearly seen in Fig. 3e and f. No interlayer gaps between ZSH, CQDs and carbon layers, confirming that CQDs and amorphous carbon layers are strongly attached to ZSH.

TEM-mapping was investigated to confirm elemental distribution of sample. Fig. 4 shows a single sphere-like composite and corresponding elements distribution including Zn, Sn, O, and C. As can be seen from Fig. 4a–c, elements of Zn, Sn and O are homogeneously distributed throughout the single micro-sphere and an obvious yolk-shell could be clearly observed. In Fig. 4d, appreciable